Kinesin-1–powered microtubule sliding initiates axonal regeneration in *Drosophila* cultured neurons

Wen Lu, Margot Lakonishok, and Vladimir I. Gelfand
Department of Cell and Molecular Biology, Feinberg School of Medicine, Northwestern University, Chicago, IL 60611

ABSTRACT **Understanding the mechanism underlying axon regeneration is of great practical importance for developing therapeutic treatment for traumatic brain and spinal cord injuries. Dramatic cytoskeleton reorganization occurs at the injury site, and microtubules have been implicated in the regeneration process. Previously we demonstrated that microtubule sliding by conventional kinesin (kinesin-1) is required for initiation of neurite outgrowth in *Drosophila* embryonic neurons and that sliding is developmentally down-regulated when neurite outgrowth is completed. Here we report that mechanical axotomy of *Drosophila* neurons in culture triggers axonal regeneration and regrowth. Regenerating neurons contain actively sliding microtubules; this sliding, like sliding during initial neurite outgrowth, is driven by kinesin-1 and is required for axonal regeneration. The injury induces a fast spike of calcium, depolymerization of microtubules near the injury site, and subsequent formation of local new microtubule arrays with mixed polarity. These events are required for reactivation of microtubule sliding at the initial stages of regeneration. Furthermore, the c-Jun N-terminal kinase pathway promotes regeneration by enhancing microtubule sliding in injured mature neurons.**

Monitoring Editor
Richard Fehon
University of Chicago

Received: Oct 2, 2014
Revised: Dec 31, 2014
Accepted: Jan 27, 2015

INTRODUCTION

Neurons are highly polarized cells with long axons extending far away from the cell body. Their length makes them highly susceptible to mechanical damage, and it is crucial for an injured neuron to regenerate its axon to recover its function. Previous work on axon regeneration in *Drosophila* neurons in vivo revealed that molecular mechanisms underlying axonal regeneration include signaling pathways and cytoskeletal reorganization (Stone *et al.*, 2010, 2012; Xiong *et al.*, 2010, 2012; Xiong and Collins, 2012; Chen *et al.*, 2012; Ghannad-Rezaie *et al.*, 2012; Song *et al.*, 2012; Klinedinst *et al.*, 2013). However, in vivo analysis does not allow for high-resolution imaging of the regeneration process and limits application of pharmacological inhibitors for the analysis of regeneration mechanisms. In this study, we developed an in vitro axotomy technique in cultured *Drosophila* neurons and manipulated the regeneration process using both *Drosophila* genetics and pharmacological drugs.

There are two occasions when major neurite outgrowth occurs: during neurogenesis from a spherical progenitor cell to a differentiated neuron, and during neuronal regeneration after injury. Previously, we demonstrated that kinesin-1–powered microtubule sliding drives initial neurite outgrowth in young neurons by pushing the peripheral membrane forward and that this sliding is developmentally down-regulated in mature neurons once neurite outgrowth is completed (Lu *et al.*, 2013b). The in vitro axotomy technique allowed us to show that axotomy induces a fast spike of Ca^{2+} that results in local depolymerization of microtubules. This depolymerization is followed by formation of new microtubule arrays of mixed polarity, leading to reactivation of kinesin-1–driven microtubule sliding and initiation of regeneration. Furthermore, we observed that sliding reactivation is modulated by c-Jun N-terminal kinase (JNK) pathway, a known stress-activated protein kinase cascade.

This article was published online ahead of print in MBoC in Press (http://www.molbiolcell.org/cgi/doi/10.1091/mbc.E14-10-1423) on February 5, 2015.

Address correspondence to: Vladimir I. Gelfand (vgelfand@northwestern.edu).

Abbreviations used: CA, constitutively active; EGTA, ethylene glycol tetraacetic acid; GFP, green fluorescent protein; JNK, c-Jun N-terminal kinase; KHC, kinesin-1 heavy chain; *puc*, *puckered*; ROI, region of interest; Syt, synaptotagmin; TIRF, total internal reflection fluorescence; UAS, upstream activation sequence.

RESULTS

Kinesin-1–powered microtubule sliding drives neurite outgrowth in injured motor neurons from the larval brain

As we previously described, kinesin-1–powered microtubule sliding drives initial neurite outgrowth in young growing neurons, but sliding mostly stops in mature neurons (Lu *et al.*, 2013b). We hypothesized that the same mechanism could be reactivated during neuronal injury, providing mechanical force for initial regeneration. We first performed an experiment to assay the role of microtubule sliding in neurons after massive damage. In *Drosophila* third-instar larvae, motor neurons extend their axons from the ventral ganglion to target muscles to form neuronal muscular junctions that control muscle movement (Figure 1, A and B; Keshishian *et al.*, 1996; Pilling *et al.*, 2006). We dissociated motor neurons from the dissected larval brains (Egger *et al.*, 2013). These motor neurons lose their neurites during dissection and dissociation (Figure 1, C and D) and therefore represent a good model of massive neuronal injury. Within 2–3 d in culture, these dissociated motor neurons regrow long (>50 µm) neurites (Figure 1E). In these long neurites, we observed active organelle transport as shown by a mitochondrial marker (upstream activation sequence [UAS]-Mito–green fluorescent protein [GFP]) under a motor neuron–specific promoter, *D42*-Gal4 (Pilling *et al.*, 2006; Supplemental Figure S1, A and A′). We expressed an axonal marker, enhanced GFP-tagged synaptotagmin (Syt-eGFP; Zhang *et al.*, 2002), in motor neurons and found that Syt-positive vesicles usually accumulated in the longest neurite (Supplemental Figure S1B). We also expressed a dendritic marker, DenMark (Nicolai *et al.*, 2010), and found that it was excluded from the longest neurite (Supplemental Figure S1C). Furthermore, we examined the microtubule polarity using an EB1-GFP construct under *D42* driver and showed that the longest neurites invariably contain microtubules of uniform polarity (plus-ends out; Supplemental Figure S1, D and D′), consistent with known polarity of microtubules in axons of motor neurons in vivo (Stone *et al.*, 2008). Taking the results together, we conclude that motor neurons dissociated from the larval brain are capable of regenerating axons (the longest neurite) in culture.

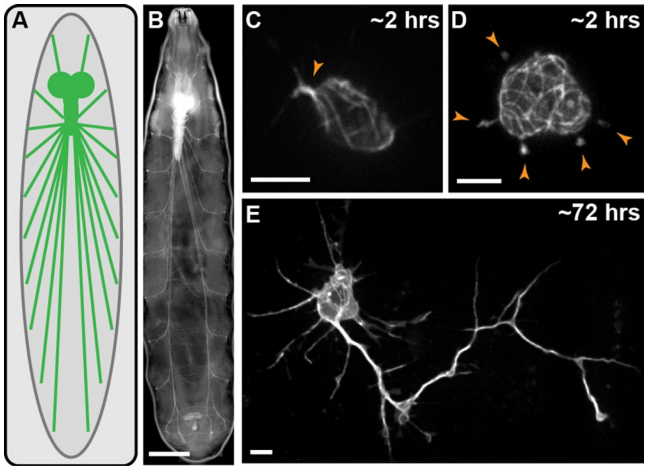

FIGURE 1: Larval motor neuron regeneration after dissociation. (A) Motor neuron pattern in a *Drosophila* third-instar larva. (B) Motor neurons in a live third-instar larva labeled with a GFP-tagged Nrv2. The larva was oriented anterior up, and the ventral side view is imaged. Scale bar, 500 µm. (C, D) Motor neurons in culture 2 h after dissociation, with only one (C) or several (D) very short neurites (gold arrowheads). Scale bar, 5 µm. (E) A motor neuron in culture for 72 h after dissociation, with a long neurite, >50 µm. Scale bar, 5 µm.

To examine microtubule movement in motor neurons after dissociation, we expressed the photoconvertible EOS-tagged α-tubulin (Lu *et al.*, 2013b) under *D42* driver and converted it in the cell body from green to red, thus applying fiduciary marks on microtubules. By following photoconverted microtubule segments in the red channel, we observed a very high level of microtubule sliding in these freshly plated (2–4 h) neurons ($N = 29$). Microtubules from the photoconverted areas penetrated the neurites and underwent extensive bending, looping, and sprouting to growing neurites (Figure 2, A and B, and Supplemental Video S1). However, after the regeneration is completed, microtubule sliding becomes undetectable both in the cell body and in neurites (Figure 2, C and D; $N = 29$; Supplemental Video S2).

As seen during initial neurogenesis, microtubule sliding is completely dependent on kinesin-1 heavy chain (KHC; Lu *et al.*, 2013b). Maternal load of wild-type KHC mRNA from *KHC* heterozygous mutant mothers allows *KHC* homozygous mutant flies to complete most of the embryonic and larval neurogenesis, until second-instar larvae, when maternally loaded mRNA gets completely depleted (Saxton *et al.*, 1991; Hurd and Saxton, 1996; Brendza *et al.*, 2000). Therefore we cultured larval brain neurons from *KHC* mutant third-instar larvae with the maternal load of KHC already depleted to address the role of KHC in regeneration. *KHC* mutant larval brain neurons have very little microtubule motility (Figure 3, A–A″, and Supplemental Video S3; $N = 20$), and all failed to regenerate axons after dissociation and plating (Figure 3, B, C, C′, and E).

Kinesin-1 in neurons is required for both organelle transport and microtubule sliding (Barlan *et al.*, 2013; Lu *et al.*, 2013b); thus inhibition of regeneration in *KHC* mutant larval brain neurons could potentially be caused by disruption of organelle transport. Therefore we also tested the role of organelle transport during regeneration. Because kinesin-1 and cytoplasmic dynein are interdependent for organelle transport (Hancock, 2014), inhibition of cytoplasmic dynein abolishes kinesin-1–mediated transport of multiple cargoes, including synaptotagmin-containing synaptic vesicles (Martin *et al.*, 1999), mitochondria (Pilling *et al.*, 2006), peroxisomes (Kural *et al.*, 2005; Ally *et al.*, 2009), neurofilaments (Uchida *et al.*, 2009), lipid droplets (Gross *et al.*, 2002; Shubeita *et al.*, 2008), and ribonucleotide granules (Ling *et al.*, 2004). We expressed RNA interference (RNAi) against the *Drosophila* dynein heavy chain (*DHC64C-RNAi*) in the larval nervous system, and this RNAi led to larval posterior paralysis and complete pupal lethality, which is similar to the phenotypes of Dhc64C transheterozygotes combining a hypomorphic allele $Dhc64C^{6-10}$ with either a *Dhc64C* deletion Df(3L)10H or an amorphic allele $Dhc64C^{4-19}$ (Martin *et al.*, 1999). Cultured *DHC64C-RNAi* larval brain neurons display no major defects in axonal outgrowth compared with control (Figure 3, B, D, and E). However, the kinesin-1–dependent mitochondrial movement in these *DHC64C-RNAi* larval brain neurons is significantly diminished compared with the control (Supplemental Figure S2, A–A″ and B–B″). Taking the results together, we conclude that the failure of regeneration in *KHC* mutant neurons does not result from inhibition of organelle transport, because *DHC-RNAi* efficiently blocks organelle transport but not axonal regeneration in larval brain neurons. These data strongly suggest that kinesin-1–powered microtubule sliding drives initial axon regeneration after traumatic axonal injury.

Microtubule sliding is activated after axotomy

To study axonal local real-time response to injury, we performed mechanical axotomy in individual neurons. We cultured neurons from dissociated gastrulation embryos (Lu *et al.*, 2013a,b) and

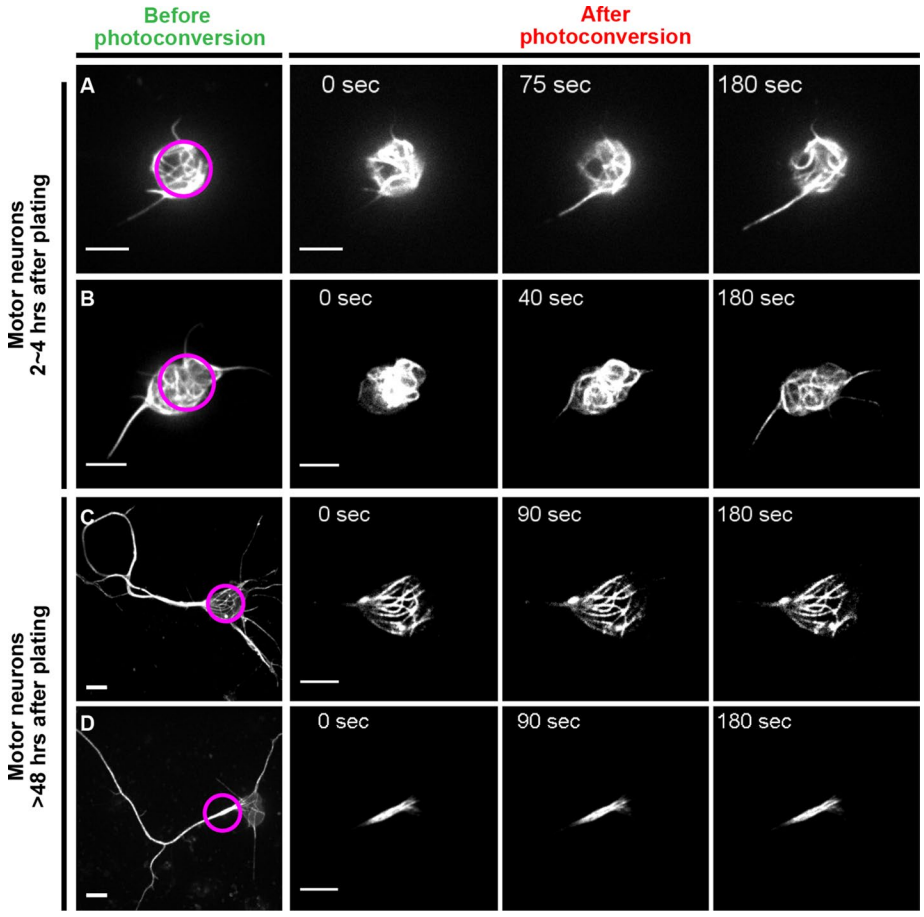

FIGURE 2: Microtubule sliding promotes neurite outgrowth during larval motor neuron regeneration. (A, B) Motor neurons expressing photoconvertible tdEOS-tagged α-tubulin 84B under the motor neuron–specific *D42* driver (*D42*>tdEOS-αtub84B) at 2–4 h in culture after plating, showing a high level of microtubule sliding. (C, D) Motor neurons (*D42*>tdEOS-αtub84B) at >48 h in culture after plating, showing no detectable microtubule sliding in the cell body (C) or in the neurite (D). Column 1 shows the green signal of tdEOS-αtub84B before photoconversion, with the photoconversion zone marked by a purple circle; columns 2–4 show the red signal of tdEOS-αtub84B after photoconversion in the indicated areas (purple circles). Note that in A and B, photoconverted microtubules move outside the photoconversion area. Scale bar, 5 μm.

removed the distal portions of axons by using a glass needle operated by a micromanipulator (see details in *Materials and Methods*; Figure 4A). We first imaged microtubules using an endogenous GFP-tagged microtubule-associated protein, Jupiter-GFP (Morin *et al.*, 2001; Karpova *et al.*, 2006; Lu *et al.*, 2013b), and found that there is little neurite outgrowth or microtubule motility in intact 4-d-old mature neurons (Supplemental Figure S3, A–C′). In contrast, after axotomy, regenerating axons contain extensively looping microtubules (Figure 4, B and B′, and Supplemental Video S4), a strong indication of microtubule sliding reactivation. Furthermore, we noticed that these microtubules pushed against the very tip of the neurite membrane during the regeneration process (compare phase images in Figure 4B to Jupiter-GFP images in Figure 4B′; Supplemental Video S4).

To visualize directly microtubule sliding, we examined photoconverted microtubule segments in neurons expressing photoconvertible tdEOS-αtub84B under a panneuronal-specific driver, *elav* (Campos *et al.*, 1987; Robinow and White, 1988), using total internal reflection fluorescence (TIRF) microscopy. We found that although there is no visible microtubule sliding in intact mature neurons (4 d in culture; Supplemental Figure S3, D and D′; Lu *et al.*, 2013b), robust sliding is reactivated after injury: the microtubule segments slide into the regenerating tips, and sliding reactivation consistently correlates with the initiation of axon outgrowth after injury (Figure 4, C–D′, orange arrowheads, and Supplemental Video S5). In addition to microtubules pushing against the tips of the growing processes, we also observed microtubules moving in the retrograde direction, implying bidirectional sliding of microtubules (Figure 4, C′ and D′, blue arrowheads, and Supplemental Video S5). Taken together, these results support the idea that microtubule sliding is reactivated by injury to initiate axonal regrowth.

Axotomy leads to a fast Ca^{2+} influx and formation of microtubules of mixed polarity

We next investigated what the initial injury signal could be from the injury site that causes the axon to regenerate. Calcium has been implicated as an essential player in the neuronal injury process (Ziv and Spira, 1995, 1997; Gitler and Spira, 1998; Kamber *et al.*, 2009; Ghosh-Roy *et al.*, 2010). We used a calcium reporter, GCaMP3 (Tian *et al.*, 2009), to monitor the intracellular calcium level upon injury. We observed a rapid calcium influx initiating at the injury site that spreads along the neurite (Figure 5, A and A′, and Supplemental Figure S4A) and reaches the cell body within seconds (Figure 5A″, Supplemental Figure S4A, and Supplemental Video S6). The calcium signal usually drops back to the normal level within 1–2 min (Figure 5A‴).

Calcium has been shown to depolymerize microtubules (Marcum *et al.*, 1978; Keith *et al.*, 1983; O′ Brien *et al.*, 1997). Therefore we wanted to determine whether microtubules are depolymerized by the calcium influx after injury. We imaged *elav*>tdEOS-αtub neurons in green channel during the axotomy procedure and found very fast microtubule disassembly in the distal axon near the injury site (Figure 5, B and B′, and Supplemental Video S7) without any significant axon retraction (Figure 5B″), whereas much less depolymerization was detected in the cell body or the proximal axon (Figure 5, B, B′, and C). We further found that the microtubules at the injury site recovered within 2 h after the fast depolymerization (Supplemental Figure S5A).

We then examined whether this calcium influx is necessary for initiation of axonal regeneration. We added 10 mM ethylene glycol tetraacetic acid (EGTA) to the medium to chelate extracellular calcium and, using *elav*>GCaMP3, demonstrated that this concentration of EGTA completely blocks calcium influx after axotomy (Supplemental Figure S4B; compare to Supplemental Figure S4A; Supplemental Video S6). We further examined microtubules upon axotomy in the presence of 10 mM EGTA and found that without the calcium influx, microtubules stay intact after injury (Figure 5C, Supplemental Figure S4, C–C‴, and Supplemental Video S7).

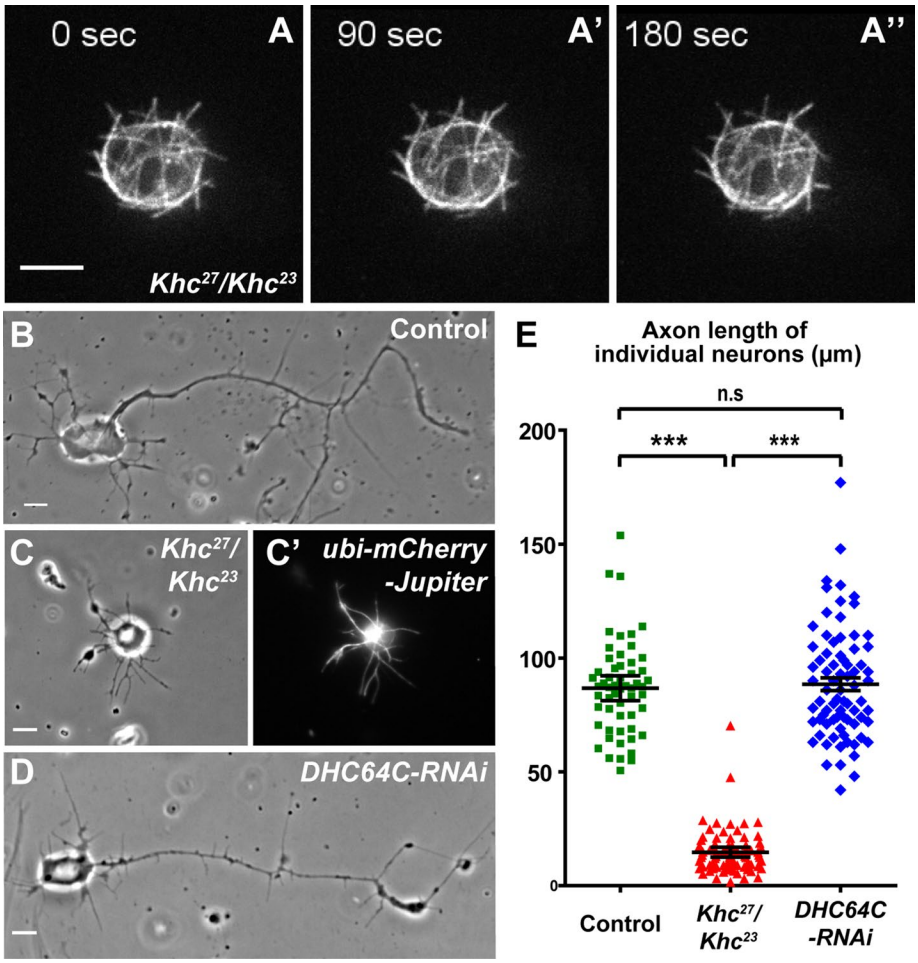

FIGURE 3: KHC drives microtubule sliding during larval neuron regeneration. (A–A″) A freshly dissociated *Khc* mutant (*Khc*^{27}/*Khc*^{23}) neuron (~2–4 h in culture after plating) has little motility of microtubules labeled by *ubi*-Jupiter-mCherry. (B) A control neuron (~72 h after plating) has a long axon. (C, C′) A *Khc* mutant (*Khc*^{27}/*Khc*^{23}) neuron (~72 h after plating) has very short neurites. (D) A *DHC64C-RNAi* mutant neuron (~72 h after plating) has a long axon. (E) Quantification of the axon length in control, *Khc* mutant (*Khc*^{27}/*Khc*^{23}), and *DHC64C-RNAi* (~72 h after plating). The average (±95% confidence interval [CI]) for the control is 86.8 ± 5.5 μm (n = 56); the average (±95% CI) for the *Khc* mutant is 14.7 ± 2.2 μm (n = 80); the average (±95% CI) for *DHC64C-RNAi* is 88.5 ± 5.6 μm (n = 76). Unpaired t test between control and *Khc* mutant neurons: ***$p < 0.0001$; unpaired t test between *Khc* mutant and *DHC64C-RNAi* neurons: ***$p < 0.0001$; unpaired t test between control and *DHC64C-RNAi* neurons: $p = 0.6693$ (nonsignificant). Scale bar, 5 μm.

Further, no regeneration can be detected after axotomy in the presence of 10 mM EGTA (Figure 6A), indicating that calcium influx after injury is necessary to initiate regeneration.

One of the possible roles of calcium during regeneration could be depolymerization and subsequent reorganization of the microtubule network. To observe directly the reorganization of the microtubule network, we used a plus-end marker, *ubi*-EB1-GFP (Shimada *et al.*, 2006), to examine microtubule orientation in axons after injury (Figure 6B). Before injury, growing microtubules have uniform polarity (plus-ends out) (Figure 6C, top). Immediately after the injury, microtubule polymerization was inhibited (Figure 6C, middle), which is consistent with our results showing fast microtubule depolymerization caused by calcium influx (Figure 5, B, B′, and C). Within 30 min after the injury, we observed formation of new microtubules, which, unlike microtubules before the injury, have mixed polarity (Figure 6C, bottom), and this unusual microtubule arrangement persists for >1 h after injury induction (Supplemental Figure S5B). This observation is in agreement with previous studies showing microtubule polarity change upon injury (Kamber *et al.*, 2009; Song *et al.*, 2012). We propose that microtubule repolymerization after Ca^{2+}-induced disassembly occurs on the residual nucleation sites without directional bias and results in the formation of new mixed-polarity microtubule arrays.

To analyze the role of microtubule depolymerization and the subsequent polarity change in the early stages of axonal regeneration, we performed axotomy in the presence of a low concentration of vinblastine (10 nM). This substoichiometric amount of the drug is sufficient to block microtubule dynamics (Supplemental Figure S6, A and B; Lu *et al.*, 2013b) but does not cause depolymerization of the existing microtubule network (Supplemental Figure S6, C and D). We observed that inhibition of microtubule dynamics by vinblastine completely prevents regeneration (Figure 6A and Supplemental Video S8). There are two possible explanations for the inhibition by vinblastine: 1) tubulin polymerization is the major force driving initial regeneration, and 2) microtubule polarity change is essential for regeneration initiation. We reasoned that since the microtubule polarity change occurs promptly after axotomy, inhibition of microtubule dynamics only at the earlier stage or only at the later stage by vinblastine would allow us to distinguish between these two possibilities. Therefore first we performed the axotomy in presence of 10 nM vinblastine and waited 2 h before we washed out the drug. This vinblastine treatment eliminated formation of mixed-polarity arrays near the injury site (Supplemental Figure S6E) and abolished regeneration (Figure 6A). Second, we added 10 nM vinblastine 3–4 h after the axotomy procedure, when formation of mixed-polarity arrays is already completed. Unlike addition of vinblastine before the time of injury, this delayed addition did not block microtubule sliding or regeneration (Figure 6A); instead, we observed microtubule looping and sprouting in the absence of microtubule dynamics (Figure 6, D–D‴, and Supplemental Video S8), which provides strong evidence of microtubule sliding after axotomy. Therefore we conclude that mixed-polarity microtubules are essential for the initiation of axonal regeneration.

Kinesin heavy chain drives sliding of mixed-polarity microtubules

We next examined whether KHC is responsible for microtubule sliding after injury, as it is during initial neurite outgrowth (Lu *et al.*, 2013b). We specifically knocked down KHC in the *Drosophila* nervous system by expressing RNAi against KHC (see *Materials and Methods*). Knockdown of KHC leads to larval growth defects, locomotion abnormality, and eventually 100% lethality before reaching

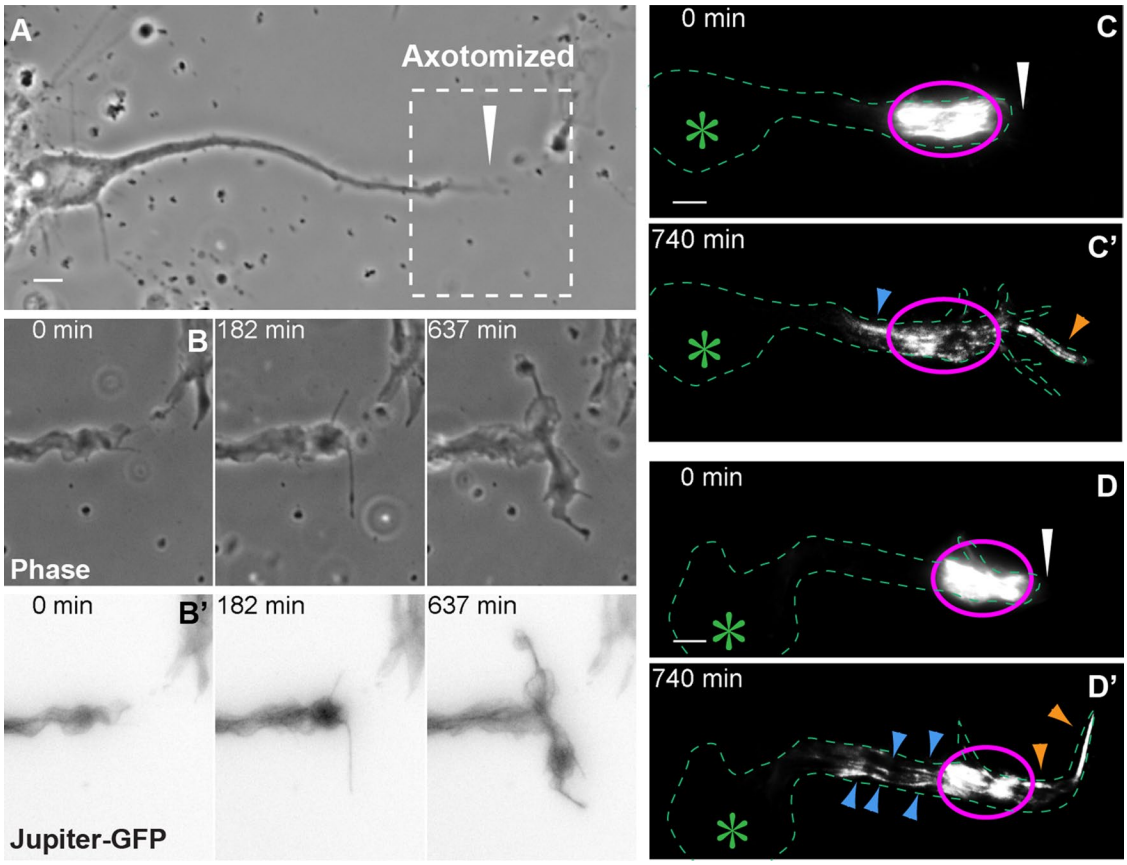

FIGURE 4: Microtubule sliding is reactivated upon axonal injury and powers axonal regrowth. (A) An embryonic Jupiter-GFP neuron after axotomy. White arrowhead shows the axotomy site. (B, B′) Different time points of the regeneration event at the axotomized tip, indicated by the white dashed box in A. (B) Phase-contrast images; (B′) inverted fluorescence images of Jupiter-GFP. (C–D′) Two examples of microtubule sliding in injured neurons expressing photoconvertible tdEOS-tagged α-tubulin 84B (*elav*>tdEOS-αtub84B). Purple circle, photoconverted area; white arrowhead, axotomy position; green dashes, outline of the cell indicated by transmitted light images (not shown); green asterisk, nucleus position; orange arrowheads, anterograde movement of photoconverted microtubules; blue arrowheads, retrograde movement of photoconverted microtubules. Scale bar, 5 μm.

the pupal stage ($N > 300$), which is similar to the phenotypes of the strongest *KHC*-null alleles (Saxton *et al.*, 1991; Hurd and Saxton, 1996). Owing to the maternal loaded KHC mRNA and KHC protein from the wild-type mothers (Saxton *et al.*, 1991; Hurd and Saxton, 1996; Brendza *et al.*, 2000), we were able to culture embryonic *KHC-RNAi* neurons that could extend axons suitable for the axotomy experiment. Because the strongest *KHC* mutant flies died at the third-instar larval stage, we estimate that the cultured 4-d-old embryonic neurons have depleted most of the maternal load of KHC mRNA and protein. Supporting this claim, a previous study demonstrated that *KHC*-mutant neurons cultured in this way have little kinesin-1–dependent organelle transport (Barlan *et al.*, 2013). We performed axotomy in these cultured 4- to 5-d-old *KHC-RNAi* neurons and found that none were able to regenerate (Figure 6A), indicating that not only is KHC essential for initial neurite outgrowth, it is also required for initiation of regeneration.

Similar to the experiments performed in larval brain neuron regeneration, we also tried to distinguish the roles of kinesin-1–mediated organelle transport and kinesin-1–powered microtubule sliding in regeneration after mechanical axotomy. To achieve this, we inhibited cytoplasmic dynein activity by a small-molecule inhibitor, ciliobrevin D (Firestone *et al.*, 2012). Owing to the interdependence of kinesin-1 and cytoplasmic dynein in bidirectional transport, ciliobrevin D treatment abolished kinesin-1–dependent mitochondrial movement (Supplemental Figure S6, F and G; Firestone *et al.*, 2012; Lu *et al.*, 2013b; Sainath and Gallo, 2014), as well as kinesin-1–dependent peroxisome transport (Firestone *et al.*, 2012). However, ciliobrevin D does not affect kinesin-1–mediated microtubule sliding (Lu *et al.*, 2013b). Therefore ciliobrevin D treatment allows us to distinguish between two roles of kinesin-1. In ciliobrevin D–treated neurons, we consistently observed regeneration events at a level comparable to control (Figure 6A). These data exclude the possibility that the failure of regeneration in *KHC-RNAi* neurons is caused by inhibition of organelle transport. Furthermore, these data indicate that kinesin-1, not cytoplasmic dynein, is the main driver of microtubule sliding during initial regeneration after axotomy.

JNK activation stimulates microtubule sliding and promotes regeneration

We showed that change of microtubule polarity caused by calcium influx is necessary for kinesin-1–powered microtubule sliding during initial regeneration. However, microtubule reorganization alone is probably not sufficient for sliding reactivation, since microtubule polarity changes occur within 30 min of axotomy, but we usually observe initial regeneration only after 2 h in culture. Therefore we further investigated the role of an injury-response signaling

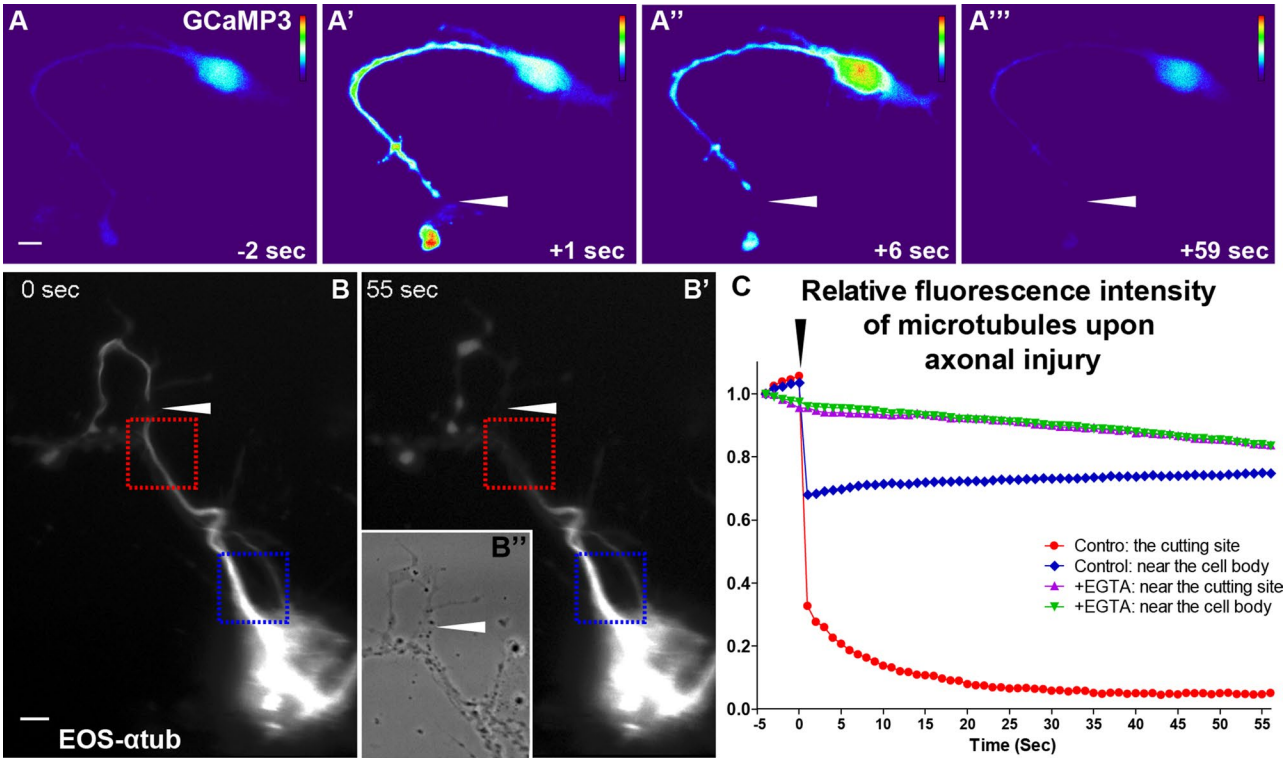

FIGURE 5: Axotomy leads to fast Ca^{2+} influx and microtubule depolymerization. (A–A‴) Signal heat maps of a neuron-specific calcium reporter (*elav*>GCaMP3) before and after axotomy, showing that a fast spike of calcium occurs upon mechanical axotomy. Axotomy is indicated by the white arrowheads (A′–A‴). (B, B′) Fast microtubule depolymerization occurs upon axonal injury in an *elav*>tdEOS-αtub84B neuron (green channel). (B″) Postcutting phase image of B′. (C) Quantification of relative fluorescence intensity of green tdEOS-αtub84B signal at two sites of the axon, near the cutting site and near the cell body, in control neurons (red and blue boxes in B and B′, respectively) and in 10 mM EGTA–treated neurons (purple and green boxes in Supplemental Figure S4 C–C‴, respectively). All intensities were normalized to the intensity of the first frame (–5 s). Axotomy occurred at 0 s, indicated as the black arrowhead. Scale bar, 5 μm.

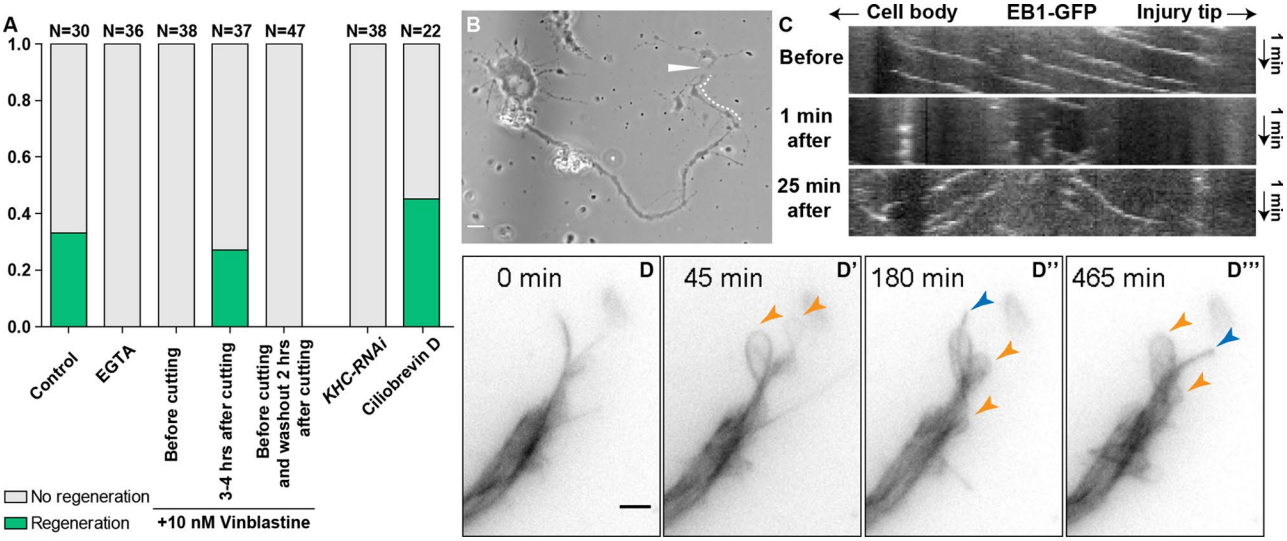

FIGURE 6: Reorganization of microtubules after axotomy. (A) Quantification of axonal regeneration percentage in control, EGTA-treated, vinblastine-treated, *elav*>*KHC-RNAi*, and ciliobrevin D–treated neurons. The *y*-axis represents the regeneration ratio (≥5-μm neurite regrowth overnight is counted as a regeneration event) of all the samples examined. (B, C) Microtubules of mixed polarity formed after axotomy. (B) A phase-contrast image of the neuron, with white arrowhead showing the axotomy site. (C) Kymographs of EB1-GFP comets in the segment of the axon next to the axotomy site marked with white dashed line in B: before (top), 1 min after (middle), and 25 min after (bottom) axotomy. (D–D‴) Inhibition of microtubule dynamics by 10 nM vinblastine 4 h after axotomy does not prevent Jupiter-GFP–labeled microtubule movement and looping. Looping microtubules are indicated by orange arrowheads, and sprouting microtubules are indicated by blue arrowheads. The time of adding 10 nM vinblastine is 0 min (120 min after imaging). Scale bar, 5 μm.

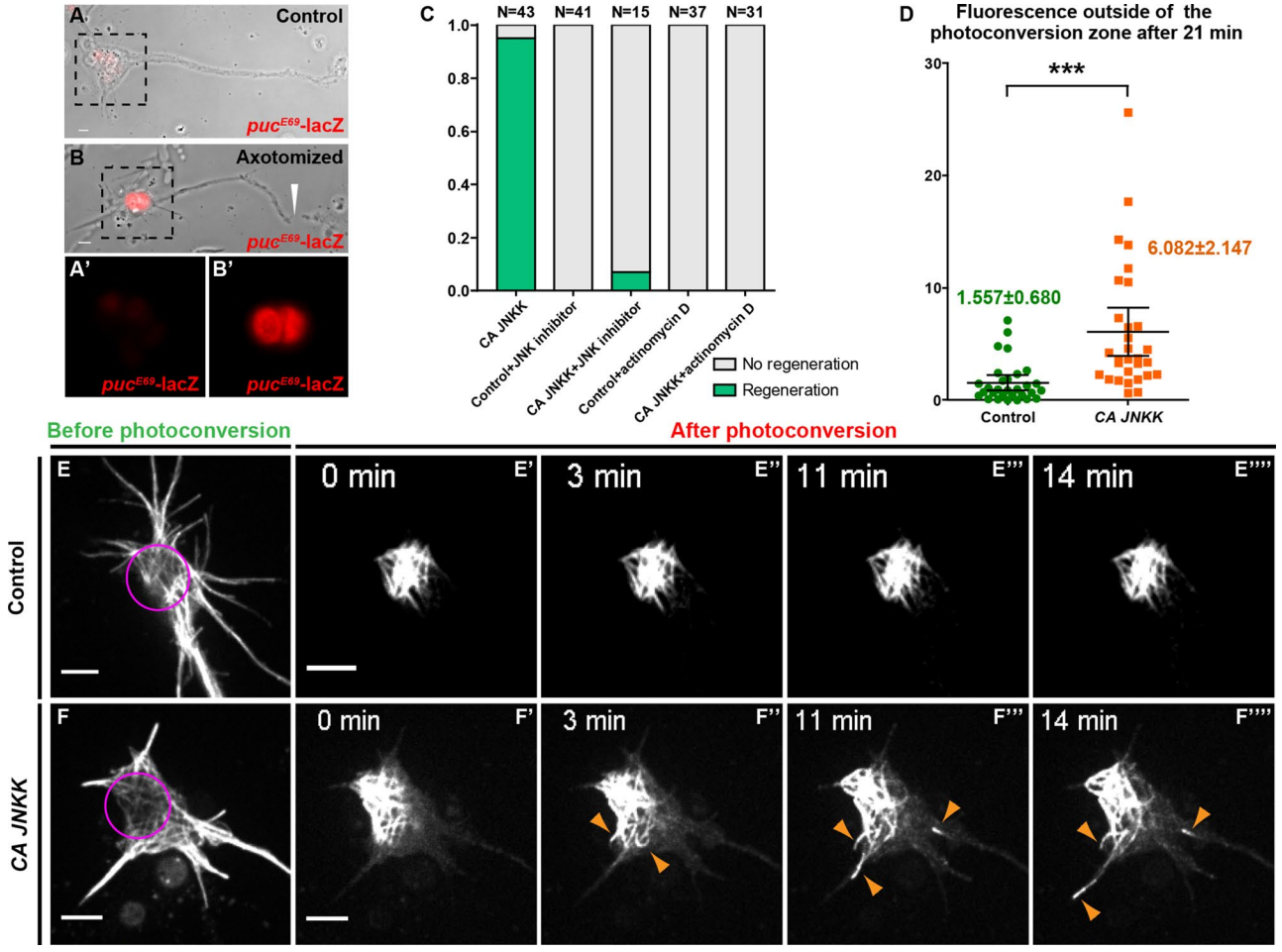

FIGURE 7: JNK regulates neuronal regeneration by enhancing microtubule sliding. (A, B) JNK pathway activity is stimulated by axonal injury. JNK transcriptional activity is visualized by an enhancer trap of JNK target gene, *puc*^{E69}-lacZ, in a control intact neuron (A) and an axotomized neuron (B). (A′, B′) Boxed area in A and B, respectively. Fluorescence images in A′ and B′ were acquired and adjusted identically. White arrowhead, axotomy position. (C) Quantification of axonal regeneration percentage in constitutively active JNK mutant (*CA JNKK*), JNK inhibitor (SP600125)-treated, and actinomycin D–treated neurons. The *y*-axis represents the regeneration ratio (≥5-μm neurite regrowth overnight is counted as a regeneration event) of all the samples examined. (D) Quantification of fluorescence signal outside of the photoconversion zone after 21 min in control and *CA JNKK* neurons, both 4 d in culture. Unpaired *t* test: $p < 0.005$. (E–E′′′′) A 4-d control neuron has no detectable microtubule sliding. (F–F′′′′) A 4-d *CA JNKK* neuron slides microtubules from the cell body to neurites (indicated by orange arrowheads). Purple circle, photoconverted area; scale bar, 5 μm.

pathway, the JNK pathway. The JNK pathway has been implicated in stress-related responses, including axon regeneration in *Drosophila* (Stone *et al.*, 2010; Xiong *et al.*, 2010; Xiong and Collins, 2012; Chen *et al.*, 2012) and other neuronal systems (Hammarlund *et al.*, 2009; Itoh *et al.*, 2009; Barnat *et al.*, 2010; Ghosh-Roy *et al.*, 2010; Nix *et al.*, 2011).

We first used an enhancer trap reporter of a JNK transcriptional target gene, *puckered* ^{E69} (*puc*^{E69})-*lacZ* (Martin-Blanco *et al.*, 1998), to assay the JNK activity in intact and injured neurons. β-Gal staining indicated that the injured neurons are characterized by a dramatic increase in JNK transcriptional activity compared with control neurons (Figure 7, A–B′), consistent with previous reports of elevated JNK activity upon injury and during regeneration (Waetzig *et al.*, 2006; Xiong *et al.*, 2010). To test whether JNK signaling promotes regeneration, we expressed a constitutively active (CA) form of *Drosophila* JNKK, *hemipterous*^{CA} (Weber *et al.*, 2000; *CA JNKK*), with Jupiter-mCherry to label microtubules (Lu *et al.*, 2013b) and found that enhanced JNK activity dramatically increased neuron survival and initial axon regeneration rate (Figure 7C), consistent with published reports (Hammarlund *et al.*, 2009; Xiong *et al.*, 2010; Nix *et al.*, 2011). In an opposite experiment, we blocked the JNK pathway with a JNK-specific inhibitor SP600125 (Bennett *et al.*, 2001) and observed inhibition of both regeneration and microtubule motility in control neurons (Figure 7C and Supplemental Figure S7, A and A′) and *CA JNKK* neurons (Figure 7C).

We noticed that *CA JNKK* mature neurons (4 d in culture) usually contained more looping and bending microtubules in the cell body and fewer bundled microtubules in the axons, which implies an enhanced level of microtubule sliding. We then examined whether JNK pathway promotes microtubule sliding in mature neurons. We observed a significantly higher level of sliding in *CA JNKK* neurons (Figure 7D). Microtubules in *CA JNKK* neurons clearly move outside of the photoconversion zone and slide into neurites (Figure 7, F–F′′′′, orange arrowheads), whereas in control

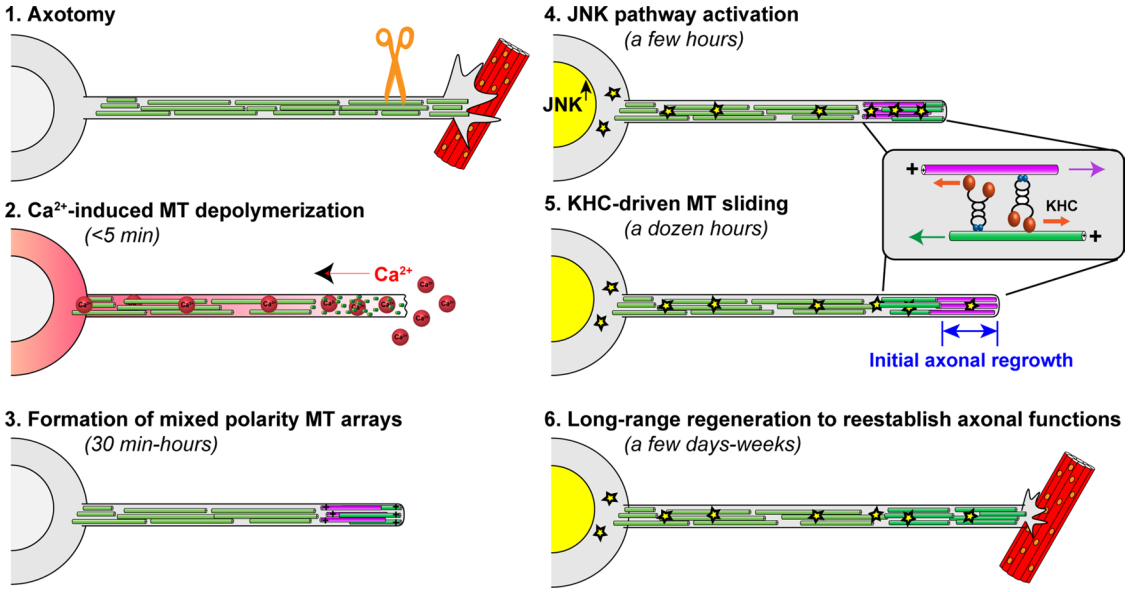

FIGURE 8: A model of initial axonal regeneration powered by KHC-driven microtubule sliding. 1) Long-extending axons are susceptible to cutting or severing by mechanical forces (axotomy). 2) Axotomy causes fast calcium–induced microtubule depolymerization near the injury site. 3) Mixed-polarity microtubule arrays are formed after the microtubule depolymerization near the injury site. 4) Axotomy activates the JNK pathway and subsequently drives transcription of key positive regulator(s) of microtubule sliding. 5) KHC slides antiparallel microtubules apart, which provides mechanical force for membrane extension during initial axonal regrowth. 6) Long-range regeneration after initial axonal regrowth reestablishes axonal functions.

neurons, microtubules show very little movement (Figure 7, E–E′′′′, and Supplemental Video S9). Therefore we conclude that JNK pathway activation stimulates microtubule sliding in mature neurons, which in turn promotes initial axonal regeneration.

JNK signaling can affect microtubule sliding and initial regeneration through two possible mechanisms: 1) JNK or another component of JNK kinase pathway could directly phosphorylate and regulate the activity of an essential regulator of microtubule sliding; 2) JNK can activate Jun/Fos-dependent transcription of a gene encoding an essential player regulating microtubule sliding. To distinguish these two mechanisms, we used a transcriptional inhibitor, actinomycin D, to stop transcriptional activity in neurons. We tested actinomycin D efficiency in cultured neurons using a RU486-inducible system (Osterwalder *et al.*, 2001; Nicholson *et al.*, 2008; Supplemental Figure S7B) and found that 10 µg/ml actinomycin D is sufficient to inhibit transcriptional activity in mature neurons (Supplemental Figure S7C; see details in *Materials and Methods*). The inhibition of transcription by actinomycin D prevents initial regeneration both in control and *CA JNKK* neurons (Figure 7C). The effect of actinomycin D on initial regeneration is not caused by cell lethality, because microtubules stay intact, and mitochondria are still moving in neurons after an overnight actinomycin D treatment (Supplemental Figure S7, D and D′, and unpublished data); this is consistent with the literature demonstrating that transcription is dispensable for survival in differentiated cultured neurons (Donady *et al.*, 1975). Furthermore, the microtubule network before and after overnight imaging appeared static (compare Supplemental Figure S7, D′ to D), implying that no microtubule sliding occurred during the imaging period. Furthermore, we examined microtubule sliding rates in cultured *Drosophila* S2 cells (Jolly *et al.*, 2010; Barlan *et al.*, 2013) immediately after actinomycin D treatment and found that there was no significant difference from control (Supplemental Figure S7E). Therefore actinomycin D does not directly inhibit microtubule sliding. Together these data indicate that JNK signaling enhances microtubule sliding and axonal regeneration through transcriptional activation.

DISCUSSION

Numerous studies of axotomy have demonstrated the importance of calcium influx, microtubule dynamics, and JNK signaling in axonal regeneration (Liu *et al.*, 2011). However, it is not clear how these factors integrate to drive axon regrowth. In this study, we showed that initial axon regeneration, like initial outgrowth of axons (Lu *et al.*, 2013b), is driven by microtubule–microtubule sliding. We demonstrated that after injury, calcium influx induces localized transient microtubule disassembly at the injury site and conversion of microtubule arrays of uniform polarity to mixed-polarity arrays. Creation of these arrays allows kinesin-1 to drive microtubule sliding and push the membrane of regenerating axons, powering their initial outgrowth (see the model in Figure 8).

In this study, we observed that axotomy induces a fast calcium influx in neurons that triggers microtubule depolymerization near the injury site, which is essential for axonal regeneration. Our observation of calcium influx upon axotomy is consistent with previous studies in several other organisms, including *Aplysia* neurons (Ziv and Spira, 1995, 1997; Kamber *et al.*, 2009), *C. elegans* sensory neurons (Ghosh-Roy *et al.*, 2010), *Drosophila* sensory neurons (Ghannad-Rezaie *et al.*, 2012), rat cortical neurons (Mandolesi *et al.*, 2004), and mouse peripheral neurons (Cho and Cavalli, 2012; Cho *et al.*, 2013). We further demonstrated that fast microtubule depolymerization near the injury site is induced by calcium influx, since chelation of Ca^{2+} by EGTA inhibits calcium influx and microtubule depolymerization, and results in failure of regeneration. We propose that this calcium-induced microtubule disassembly is the first step in creating microtubule arrays of mixed polarity in the distal axons, which could be the initial injury signal for neuronal regeneration.

Our description of microtubule dynamics in regenerating *Drosophila* axons is in agreement with previous reports that have

demonstrated dramatic reorganization of microtubules after axonal damage in several other organisms. In *Aplysia* neurons, axotomy causes reorganization of microtubules (Kamber *et al.*, 2009), and formation of microtubule-filled filopodia-like protrusions (Goldberg and Burmeister, 1992). In *C. elegans* posterior lateral microtubule (PLM) sensory neurons, microtubule growth after axonal injury is stimulated by down-regulation of depolymerizing Kinesin-13 family member KLP-7, and persistent microtubule growth is supported by elevating Δ2 posttranslational modification of α-tubulin (Ghosh-Roy *et al.*, 2012). In *Drosophila* sensory neurons, global up-regulation of microtubule dynamics and mixed microtubule orientation in dendrites have been documented after axotomy (Stone *et al.*, 2010; Chen *et al.*, 2012; Song *et al.*, 2012). In mouse peripheral neurons, tubulin near the injury site has to be deacetylated by the Histone Deacetylase 5 (HDAC5) to initiate axonal regeneration (Cho and Cavalli, 2012). In rat sensory DRG (dorsal root ganglion) neurons, the kinesin-2 family member KIF3C has been implicated as a microtubule-destabilizing factor that is essential for axonal regeneration (Gumy *et al.*, 2013).

Here we showed that formation of mixed microtubule orientation through fast microtubule depolymerization and subsequent repolymerization are required for initial axonal regeneration. Stabilization of microtubules by treatment with a low concentration of Vinblastine prevents their depolymerization and subsequent microtubule polarity change, and suppresses regeneration, while Vinblastine added after initial polarity orientation change does not affect regeneration. In our previous studies (Jolly *et al.*, 2010; Lu *et al.*, 2013b), we proposed that KHC drives microtubule-microtubule sliding by using its C-terminal tail to bind one microtubule (Hackney and Stock, 2000; Seeger and Rice, 2010), while using its processive motor domain to move along another microtubule. Since there are no signs of positive cooperatively binding of the KHC tails to microtubules in either S2 cells (our unpublished data) or in mammalian cells (Navone *et al.*, 1992), we speculate that KHC binds to two microtubules through its motor and tail domains in a random orientation. Furthermore, a recent study from our lab has demonstrated that mitotic kinesin-6, Pav/KLP, known to cross-link antiparallel microtubules at mitotic spindles (Adams *et al.*, 1998), downregulates microtubule sliding in both S2 cells and *Drosophila* neurons in vitro and in vivo (del Castillo *et al.*, 2015). Therefore we propose that an antiparallel arrangement of microtubules is required for effective KHC sliding (Figure 8). Formation of mixed polarity microtubules in axotomized axons allows KHC to slide these microtubules apart, and this process provides the mechanical force necessary to generate membrane protrusion for initial axonal regrowth. Therefore our data not only are consistent with previous reports on microtubule destabilization, enhanced dynamics, and reorganization of polarity after axotomy, but also provide a unifying mechanism explaining the requirement for microtubule reorganization. Furthermore, the C-terminal domain of KHC involved in microtubule-microtubule sliding is evolutionary conserved across the animal kingdom (Hackney and Stock, 2000; Seeger and Rice, 2010), and general changes in microtubule dynamics are characteristic of axonal regeneration in many organisms. We propose that the microtubule-sliding mechanism uncovered in this work for initial regeneration in *Drosophila* neurons also functions in the neuronal injury response in higher organisms.

Although microtubule reorganization, induced by changes in microtubule polymerization and polarity, is required for regeneration, the reorganization alone is not sufficient to activate Kinesin-1-driven microtubule sliding and injury-induced axonal regrowth. In this study, we revealed that JNK signaling promotes microtubule sliding to provide mechanical force for initial regeneration. The JNK pathway and its upstream mitogen-activated-protein kinase (MAPK) cascade have been implicated as an essential regeneration-regulating mechanism in multiple neuronal systems, including *Caenorhabditis elegans* motor neurons (Hammarlund *et al.*, 2009; Nix *et al.*, 2011; Ghosh-Roy *et al.*, 2012), *Drosophila* motor (Xiong *et al.*, 2010; Xiong and Collins, 2012) and sensory (Stone *et al.*, 2010; Chen *et al.*, 2012) neurons, and adult mouse dorsal root ganglion (DRG) neurons (Itoh *et al.*, 2009; Barnat *et al.*, 2010). Our results indicate that JNK involvement in initial axonal regeneration is dependent on its transcriptional activation. We documented that JNK signaling increases microtubule sliding in mature neurons, and this elevated level of sliding microtubule provides mechanical force for initiation of regenerating protrusions. However, it is likely that additional factors downstream of JNK transcription activation, together with microtubule sliding, contribute to long-range axonal regeneration (Figure 8). It has been shown that JNK signaling promotes stem cell maintenance in a transcription-dependent manner in *Drosophila* (Lu *et al.*, 2012), and therefore it is tempting to propose that JNK signaling could reprogram the mature neurons back to a less-differentiated status through transcriptional activation to reinitiate neurite outgrowth. Further studies on JNK transcriptional target genes involved in microtubule sliding and examination of JNK-promoting microtubule sliding in neurons of higher organisms will provide more insight into the mechanism of initial axonal regeneration, as well as aid in the development of effective therapeutic treatments for spinal cord injury and brain damage.

MATERIALS AND METHODS

Drosophila genetics

Fly stocks and crosses were kept on regular cornmeal food supplemented with dry active yeast at room temperature (~22°C) and switched to apple juice agar food supplemented with dry active yeast 2–3 d before embryo collection. For larval motor neuron regeneration experiments, *D42*-Gal4 (Pilling *et al.*, 2006) was used to specifically drive UAS expression in motor neurons. For embryonic neuron regeneration experiments, *elav*-Gal4 (Campos *et al.*, 1987; Robinow and White, 1988) was used to drive UAS expression in the nervous system. To knock down KHC in larval brain neurons, transheterozygote Khc^{27}/Khc^{23} flies (Brendza *et al.*, 1999, 2000; Serbus *et al.*, 2005) were used. To knock down DHC in larval brain neurons, a TRiP RNAi line (Bloomington stock #36583, encoding a short RNA hairpin against the DHC64C CDS 10044-10064) was driven by *elav*-Gal4. To knock down KHC in mature embryonic neurons, a TRiP RNAi line (Bloomington stock #35770, encoding a short RNA hairpin against the KHC 3′ UTR 231–251) was driven by *elav*-Gal4.

Larval motor neuron culture

The protocol is modified based on the protocol from the Sprecher lab (Egger *et al.*, 2013). *Drosophila* third-instar larvae were picked and washed with distilled H_2O, 70% EtOH, and sterile 1× modified dissection saline (9.9 mM 4-(2-hydroxyethyl)-1-piperazineethanesulfonic acid, pH 7.5, 137 mM NaCl, 5.4 mM KCl, 0.17 mM NaH_2PO_4, 0.22 mM KH_2PO_4, 3.3 mM glucose, 43.8 mM sucrose). Optic lobes and ventral ganglion were dissected and cleaned in sterile 1× modified dissection saline; tissues were then dissociated in Liberase solution (Roche, Basel, Switzerland; Liberase TM Research Grade, 05401119001, stock solution 2.5 mg/ml 13 Wünsch units/ml in sterile 1× modified dissection saline, final concentration in 0.25 mg/ml 1.3 Wünsch units/ml) for 1 h. The neurons were spun down at 300 × *g* for 5 min and then washed twice in supplemented

Schneider's medium (20% fetal bovine serum, 5 µg/ml insulin, 100 µg/ml penicillin, 100 µg/ml streptomycin, and 10 µg/ml tetracycline); the neurons were plated onto concanavalin A–coated coverslips and allowed attached for 30 min before addition of full volume of supplemented Schneider's medium for imaging 2–4 h after plating or incubated for 2–3 d before imaging.

Embryonic neuronal axotomy procedure

The detailed embryonic neuronal preparation protocol is available online (www.jove.com/video/50838/organelle-transport-cultured-drosophila-cells-s2-cell-line-primary; Lu *et al.*, 2013a). Cultured embryonic neurons were kept in 25°C in an insect cell incubator for 4–5 d in supplemented Schneider's medium with 5 µM cytochalasin D; cytochalasin D was then washed out and 50 µg/ml gentamicin added for the axotomy experiment. A fine glass needle was prepared from a borosilicate glass capillary (outer diameter, 1.00 mm; inner diameter, 0.78 mm) using a Flaming/Brown Micropipette Puller (model P-97, Sutter Instrument, Novato, CA) and manually controlled by a Nikon Narishige (Tokyo, Japan) micromanipulator. The needle tip usually scratches against the axon perpendicularly once or twice to complete the axotomy. As indicated, the following drugs were added to cultured neurons before the axotomy procedure: EGTA (10 mM), vinblastine (10 nM), ciliobrevin D (20 µM), SP600125 (20 µM), and actinomycin D (10 µg/ml).

Microscope image acquisition

A Nikon (Tokyo, Japan) Eclipse U2000 inverted microscope equipped with S-Flor 40×/1.30 numerical aperture (NA) and Plan-Apo 100×/1.4 NA objectives was used to perform neuronal axotomy and image regeneration. Images were acquired by a digital complementary metal–oxide–semiconductor camera, ORCA-Flash4.0 V2 C11440-22CU (Hamamatsu Photonics, Hamamatsu, Japan) controlled by MetaMorph software, version 7.7.7.0 (Molecular Devices, Sunnyvale, CA). Phase-contrast images were obtained using a 100-W halogen lamp or CoolLED PrecisExcite (Hampshire, UK), and fluorescence excitation was achieved using an Aura light engine (Lumencor, Beaverton, OR) or X-Cite XLED (Lumen Dynamics, Mississauga, Canada). tdEOS-αtub neurons were photoconverted by ultraviolet light from a mercury light source through a pinhole in the light path for 3 s. TIRF images after photoconversion were acquired with a Plan-Apo TIRF 100×/1.45 NA lens and a Sapphire 561-nm laser (Coherent, Santa Clara, CA). A Nikon Eclipse U2000 inverted stand with a Yokogawa CSU10 spinning disk confocal head and a 100×/1.45 NA lens were used to image nonaxotomy samples. Images were acquired using an Evolve 512 electron-multiplying charge-coupled device camera (Photometrics, Tucson, AZ) controlled by Nikon NIS-Elements software (AR 4.00.07 64bt). Photoconversion of tdEOS-αtub was performed using illumination from a Heliophor 89 North light (Burlington, VT) in the epifluorescence pathway by a 405-nm filter and confined by an adjustable pinhole in the field diaphragm position (projected as an ~6- to 7-µm-diameter circle in the sample plane) for 6 s. All neurons were imaged in 20% fetal bovine serum–supplemented Schneider's medium (Sigma-Aldrich, St. Louis, MO), except for the ciliobrevin D treatment experiments, for which imaging was in nonsupplemented Schneider's medium. S2 cells were imaged in GIBCO Insect Xpress medium (Life Technologies, Carlsbad, CA). All Images were acquired in 16-bit format at room temperature (~24°C), analyzed by FIJI/ImageJ, and plotted in GraphPad Prism 5. Heat-map images of the calcium reporter (GCaMP3) were created using the ImageJ Heatmap Histogram plug-in (www.samuelpean.com/heatmap-histogram/). tdEOS-αtub84B images were bleach corrected using the ImageJ Bleach Correction plug-in (fiji.sc/Bleach_Correction). All figures were assembled in Adobe Illustrator CS4, and all videos were assembled in AVS Video Editor 5.1.

Immunochemistry for *puc*^{E69}-lacZ

Embryonic neurons from the embryos of *puc*^{E69}-lacZ/*TM6B* were plated on concanavalin A–coated, 25-mm photoetched coverslips (#72265-25; Electron Microscopy Sciences, Hatfield, PA) for >48 h. Neurons were first injured by a glass needle (see *Embryonic neuronal axotomy procedure* for more details) with the position information recorded according to the grids. After axotomy, neurons were cultured overnight (>16 h) to allow the expression of the reporter. Then neurons were washed three times in 1× phosphate-buffered saline (PBS) before fixation in 4% formaldehyde for 10 min at room temperature and then washed three times in 1× PBS and washed and blocked in wash solution (0.1% Triton X-100, 1% bovine serum albumin in Tris-buffered saline) for 10 min three times. Then they were incubated with the primary antibody, a monoclonal anti–β-galactosidase antibody (1:250; Cat# Z3781; Promega, Madison, WI), for 45 min at room temperature in a moisture chamber, washed and blocked in wash solution 10 min three times, incubated with secondary antibody, goat anti-mouse tetramethylrhodamine isothiocyanate (1:200; Jackson ImmunoResearch, West Grove, PA) for 45 min to 1 h in the dark at room temperature, and washed and blocked in wash solution 10 min three times. Cells were covered with 1× PBS and imaged directly according to the grid position information.

Quantification of fluorescence intensity of microtubules

Time-lapse movies of *elav*>tdEOS-αtub neurons (X-Cite 460 channel) were aligned using the StackReg plug-in (hbigwww.epfl.ch/thevenaz/stackreg/). Same-size regions of interest (ROIs) were assigned to different positions using ROI Manager, and the fluorescence intensity of designated ROIs over time (multimeasure in ROI Manager) was measured. Background noise was subtracted from the raw data, and the intensities of all frames were normalized according to the intensity of the first frame. The data were analyzed and plotted in GraphPad Prism 5.

Test of actinomycin D efficiency

Four identical samples of primary embryonic neurons were prepared from embryos expressing *elav.GeneSwitch*>*mCD8-GFP*. Sample 1 was treated with only dimethyl sulfoxide. Samples 2–4 were bathed in 50 µg/ml RU486 for 3 min and washed three times by supplemented Schneider's medium. Samples 3 and 4 were then treated overnight with 10 and 5 µg/ml actinomycin D, respectively. After 18 h of incubation, samples 1–4 were imaged to determine the percentage of GFP-positive neurons.

ACKNOWLEDGMENTS

We acknowledge the Bloomington *Drosophila* Stock Center, the Yale GFP Protein Trap Database, Chris Q. Doe, Isabel M. Palacios, Stephen L. Rogers, and Aaron DiAntonio for fly stocks. We thank Matt Pecot (Department of Neuroscience, Harvard University) and Liming Tan from Larry Zipursky's lab (UCLA) for sharing the larval brain dissociation protocol. Special thanks go to Kari Barlan (University of Chicago) and Michael Winding (Northwestern University) for critical reading of the manuscript. We also thank the Gelfand lab members for support and discussions. Research reported here was supported by National Institute of General Medical Science/National Institutes of Health Award R01 GM052111.

REFERENCES

Adams RR, Tavares AA, Salzberg A, Bellen HJ, Glover DM (1998). pavarotti encodes a kinesin-like protein required to organize the central spindle and contractile ring for cytokinesis. Genes Dev 12, 1483–1494.

Ally S, Larson AG, Barlan K, Rice SE, Gelfand VI (2009). Opposite-polarity motors activate one another to trigger cargo transport in live cells. J Cell Biol 187, 1071–1082.

Barlan K, Lu W, Gelfand VI (2013). The microtubule-binding protein ensconsin is an essential cofactor of kinesin-1. Curr Biol 23, 317–322.

Barnat M, Enslen H, Propst F, Davis RJ, Soares S, Nothias F (2010). Distinct roles of c-Jun N-terminal kinase isoforms in neurite initiation and elongation during axonal regeneration. J Neurosci 30, 7804–7816.

Bennett BL, Sasaki DT, Murray BW, O' Leary EC, Sakata ST, Xu W, Leisten JC, Motiwala A, Pierce S, Satoh Y, *et al.* (2001). SP600125, an anthrapyrazolone inhibitor of Jun N-terminal kinase. Proc Natl Acad Sci USA 98, 13681–13686.

Brendza KM, Rose DJ, Gilbert SP, Saxton WM (1999). Lethal kinesin mutations reveal amino acids important for ATPase activation and structural coupling. J Biol Chem 274, 31506–31514.

Brendza RP, Serbus LR, Duffy JB, Saxton WM (2000). A function for kinesin I in the posterior transport of oskar mRNA and Staufen protein. Science 289, 2120–2122.

Campos AR, Rosen DR, Robinow SN, White K (1987). Molecular analysis of the locus elav in Drosophila melanogaster: a gene whose embryonic expression is neural specific. EMBO J 6, 425–431.

Chen L, Stone MC, Tao J, Rolls MM (2012). Axon injury and stress trigger a microtubule-based neuroprotective pathway. Proc Natl Acad Sci USA 109, 11842–11847.

Cho Y, Cavalli V (2012). HDAC5 is a novel injury-regulated tubulin deacetylase controlling axon regeneration. EMBO J 31, 3063–3078.

Cho Y, Sloutsky R, Naegle KM, Cavalli V (2013). Injury-induced HDAC5 nuclear export is essential for axon regeneration. Cell 155, 894–908.

Del Castillo U, Lu W, Winding M, Lakonishok M, Gelfand VI (2015). Pavarotti/MKLP1 regulates microtubule sliding and neurite outgrowth in Drosophila neurons. Curr Biol 25, 200–205.

Donady JJ, Seecof RL, Dewhurst S (1975). Actinomycin D-sensitive periods in the differentiation of Drosophila neurons and muscle cells in vitro. Differentiation 4, 9–14.

Egger B, van Giesen L, Moraru M, Sprecher SG (2013). In vitro imaging of primary neural cell culture from Drosophila. Nat Protoc 8, 958–965.

Firestone AJ, Weinger JS, Maldonado M, Barlan K, Langston LD, O'Donnell M, Gelfand VI, Kapoor TM, Chen JK (2012). Small-molecule inhibitors of the AAA+ ATPase motor cytoplasmic dynein. Nature 484, 125–129.

Ghannad-Rezaie M, Wang X, Mishra B, Collins C, Chronis N (2012). Microfluidic chips for in vivo imaging of cellular responses to neural injury in Drosophila larvae. PLoS One 7, e29869.

Ghosh-Roy A, Goncharov A, Jin Y, Chisholm AD (2012). Kinesin-13 and tubulin posttranslational modifications regulate microtubule growth in axon regeneration. Dev Cell 23, 716–728.

Ghosh-Roy A, Wu Z, Goncharov A, Jin Y, Chisholm AD (2010). Calcium and cyclic AMP promote axonal regeneration in Caenorhabditis elegans and require DLK-1 kinase. J Neurosci 30, 3175–3183.

Gitler D, Spira ME (1998). Real time imaging of calcium-induced localized proteolytic activity after axotomy and its relation to growth cone formation. Neuron 20, 1123–1135.

Goldberg DJ, Burmeister DW (1992). Microtubule-based filopodium-like protrusions form after axotomy. J Neurosci 12, 4800–4807.

Gross SP, Welte MA, Block SM, Wieschaus EF (2002). Coordination of opposite-polarity microtubule motors. J Cell Biol 156, 715–724.

Gumy LF, Chew DJ, Tortosa E, Katrukha EA, Kapitein LC, Tolkovsky AM, Hoogenraad CC, Fawcett JW (2013). The Kinesin-2 family member KIF3C regulates microtubule dynamics and is required for axon growth and regeneration. J Neurosci 33, 11329–11345.

Hackney DD, Stock MF (2000). Kinesin's IAK tail domain inhibits initial microtubule-stimulated ADP release. Nat Cell Biol 2, 257–260.

Hammarlund M, Nix P, Hauth L, Jorgensen EM, Bastiani M (2009). Axon regeneration requires a conserved MAP kinase pathway. Science 323, 802–806.

Hancock WO (2014). Bidirectional cargo transport: moving beyond tug of war. Nat Rev Mol Cell Biol 15, 615–628.

Hurd DD, Saxton WM (1996). Kinesin mutations cause motor neuron disease phenotypes by disrupting fast axonal transport in Drosophila. Genetics 144, 1075–1085.

Itoh A, Horiuchi M, Bannerman P, Pleasure D, Itoh T (2009). Impaired regenerative response of primary sensory neurons in ZPK/DLK gene-trap mice. Biochem Biophys Res Commun 383, 258–262.

Jolly AL, Kim H, Srinivasan D, Lakonishok M, Larson AG, Gelfand VI (2010). Kinesin-1 heavy chain mediates microtubule sliding to drive changes in cell shape. Proc Natl Acad Sci USA 107, 12151–12156.

Kamber D, Erez H, Spira ME (2009). Local calcium-dependent mechanisms determine whether a cut axonal end assembles a retarded endbulb or competent growth cone. Exp Neurol 219, 112–125.

Karpova N, Bobinnec Y, Fouix S, Huitorel P, Debec A (2006). Jupiter, a new Drosophila protein associated with microtubules. Cell Motil Cytoskeleton 63, 301–312.

Keith C, DiPaola M, Maxfield FR, Shelanski ML (1983). Microinjection of Ca++-calmodulin causes a localized depolymerization of microtubules. J Cell Biol 97, 1918–1924.

Keshishian H, Broadie K, Chiba A, Bate M (1996). The Drosophila neuromuscular junction: a model system for studying synaptic development and function. Annu Rev Neurosci 19, 545–575.

Klinedinst S, Wang X, Xiong X, Haenfler JM, Collins CA (2013). Independent pathways downstream of the Wnd/DLK MAPKKK regulate synaptic structure, axonal transport, and injury signaling. J Neurosci 33, 12764–12778.

Kural C, Kim H, Syed S, Goshima G, Gelfand VI, Selvin PR (2005). Kinesin and dynein move a peroxisome in vivo: a tug-of-war or coordinated movement? Science 308, 1469–1472.

Ling SC, Fahrner PS, Greenough WT, Gelfand VI (2004). Transport of Drosophila fragile X mental retardation protein-containing ribonucleoprotein granules by kinesin-1 and cytoplasmic dynein. Proc Natl Acad Sci USA 101, 17428–17433.

Liu K, Tedeschi A, Park KK, He Z (2011). Neuronal intrinsic mechanisms of axon regeneration. Annu Rev Neurosci 34, 131–152.

Lu W, Casanueva MO, Mahowald AP, Kato M, Lauterbach D, Ferguson EL (2012). Niche-associated activation of rac promotes the asymmetric division of Drosophila female germline stem cells. PLoS Biol 10, e1001357.

Lu W, Del Castillo U, Gelfand VI (2013a). Organelle transport in cultured Drosophila cells: s2 cell line and primary neurons. J Vis Exp 81, e50838.

Lu W, Fox P, Lakonishok M, Davidson MW, Gelfand VI (2013b). Initial neurite outgrowth in Drosophila neurons is driven by kinesin-powered microtubule sliding. Curr Biol 23, 1018–1023.

Mandolesi G, Madeddu F, Bozzi Y, Maffei L, Ratto GM (2004). Acute physiological response of mammalian central neurons to axotomy: ionic regulation and electrical activity. FASEB J 18, 1934–1936.

Marcum JM, Dedman JR, Brinkley BR, Means AR (1978). Control of microtubule assembly-disassembly by calcium-dependent regulator protein. Proc Natl Acad Sci USA 75, 3771–3775.

Martin M, Iyadurai SJ, Gassman A, Gindhart JG Jr, Hays TS, Saxton WM (1999). Cytoplasmic dynein, the dynactin complex, and kinesin are interdependent and essential for fast axonal transport. Mol Biol Cell 10, 3717–3728.

Martin-Blanco E, Gampel A, Ring J, Virdee K, Kirov N, Tolkovsky AM, Martinez-Arias A (1998). puckered encodes a phosphatase that mediates a feedback loop regulating JNK activity during dorsal closure in Drosophila. Genes Dev 12, 557–570.

Morin X, Daneman R, Zavortink M, Chia W (2001). A protein trap strategy to detect GFP-tagged proteins expressed from their endogenous loci in Drosophila. Proc Natl Acad Sci USA 98, 15050–15055.

Navone F, Niclas J, Hom-Booher N, Sparks L, Bernstein HD, McCaffrey G, Vale RD (1992). Cloning and expression of a human kinesin heavy chain gene: interaction of the COOH-terminal domain with cytoplasmic microtubules in transfected CV-1 cells. J Cell Biol 117, 1263–1275.

Nicholson L, Singh GK, Osterwalder T, Roman GW, Davis RL, Keshishian H (2008). Spatial and temporal control of gene expression in Drosophila using the inducible GeneSwitch GAL4 system. I. Screen for larval nervous system drivers. Genetics 178, 215–234.

Nicolai LJ, Ramaekers A, Raemaekers T, Drozdzecki A, Mauss AS, Yan J, Landgraf M, Annaert W, Hassan BA (2010). Genetically encoded dendritic marker sheds light on neuronal connectivity in Drosophila. Proc Natl Acad Sci USA 107, 20553–20558.

Nix P, Hisamoto N, Matsumoto K, Bastiani M (2011). Axon regeneration requires coordinate activation of p38 and JNK MAPK pathways. Proc Natl Acad Sci USA 108, 10738–10743.

O'Brien ET, Salmon ED, Erickson HP (1997). How calcium causes microtubule depolymerization. Cell Motil Cytoskeleton 36, 125–135.

Osterwalder T, Yoon KS, White BH, Keshishian H (2001). A conditional tissue-specific transgene expression system using inducible GAL4. Proc Natl Acad Sci USA 98, 12596–12601.

Pilling AD, Horiuchi D, Lively CM, Saxton WM (2006). Kinesin-1 and Dynein are the primary motors for fast transport of mitochondria in Drosophila motor axons. Mol Biol Cell 17, 2057–2068.

Robinow S, White K (1988). The locus elav of Drosophila melanogaster is expressed in neurons at all developmental stages. Dev Biol 126, 294–303.
Sainath R, Gallo G (2014). The dynein inhibitor Ciliobrevin D inhibits the bidirectional transport of organelles along sensory axons and impairs NGF-mediated regulation of growth cones and axon branches. Dev Neurobiol, doi: 10.1002/dneu.22246.
Saxton WM, Hicks J, Goldstein LS, Raff EC (1991). Kinesin heavy chain is essential for viability and neuromuscular functions in Drosophila, but mutants show no defects in mitosis. Cell 64, 1093–1102.
Seeger MA, Rice SE (2010). Microtubule-associated protein-like binding of the kinesin-1 tail to microtubules. J Biol Chem 285, 8155–8162.
Serbus LR, Cha BJ, Theurkauf WE, Saxton WM (2005). Dynein and the actin cytoskeleton control kinesin-driven cytoplasmic streaming in Drosophila oocytes. Development 132, 3743–3752.
Shimada Y, Yonemura S, Ohkura H, Strutt D, Uemura T (2006). Polarized transport of Frizzled along the planar microtubule arrays in Drosophila wing epithelium. Dev Cell 10, 209–222.
Shubeita GT, Tran SL, Xu J, Vershinin M, Cermelli S, Cotton SL, Welte MA, Gross SP (2008). Consequences of motor copy number on the intracellular transport of kinesin-1-driven lipid droplets. Cell 135, 1098–1107.
Song Y, Ori-McKenney KM, Zheng Y, Han C, Jan LY, Jan YN (2012). Regeneration of Drosophila sensory neuron axons and dendrites is regulated by the Akt pathway involving Pten and microRNA bantam. Genes Dev 26, 1612–1625.
Stone MC, Nguyen MM, Tao J, Allender DL, Rolls MM (2010). Global up-regulation of microtubule dynamics and polarity reversal during regeneration of an axon from a dendrite. Mol Biol Cell 21, 767–777.
Stone M C, Rao K, Gheres Kyle W, Kim S, Tao J, La Rochelle C, Folker Christin T, Sherwood Nina T, Rolls Melissa M (2012). Normal spastin gene dosage is specifically required for axon regeneration. Cell Rep 2, 1340–1350.
Stone MC, Roegiers F, Rolls MM (2008). Microtubules have opposite orientation in axons and dendrites of Drosophila neurons. Mol Biol Cell 19, 4122–4129.
Tian L, Hires SA, Mao T, Huber D, Chiappe ME, Chalasani SH, Petreanu L, Akerboom J, McKinney SA, Schreiter ER, *et al.* (2009). Imaging neural activity in worms, flies and mice with improved GCaMP calcium indicators. Nat Methods 6, 875–881.
Uchida A, Alami NH, Brown A (2009). Tight functional coupling of kinesin-1A and dynein motors in the bidirectional transport of neurofilaments. Mol Biol Cell 20, 4997–5006.
Waetzig V, Zhao Y, Herdegen T (2006). The bright side of JNKs—multitalented mediators in neuronal sprouting, brain development and nerve fiber regeneration. Prog Neurobiol 80, 84–97.
Weber U, Paricio N, Mlodzik M (2000). Jun mediates Frizzled-induced R3/R4 cell fate distinction and planar polarity determination in the Drosophila eye. Development 127, 3619–3629.
Xiong X, Collins CA (2012). A conditioning lesion protects axons from degeneration via the Wallenda/DLK MAP kinase signaling cascade. J Neurosci 32, 610–615.
Xiong X, Hao Y, Sun K, Li J, Li X, Mishra B, Soppina P, Wu C, Hume RI, Collins CA (2012). The Highwire ubiquitin ligase promotes axonal degeneration by tuning levels of Nmnat protein. PLoS Biol 10, e1001440.
Xiong X, Wang X, Ewanek R, Bhat P, Diantonio A, Collins CA (2010). Protein turnover of the Wallenda/DLK kinase regulates a retrograde response to axonal injury. J Cell Biol 191, 211–223.
Zhang YQ, Rodesch CK, Broadie K (2002). Living synaptic vesicle marker: synaptotagmin-GFP. Genesis 34, 142–145.
Ziv NE, Spira ME (1995). Axotomy induces a transient and localized elevation of the free intracellular calcium concentration to the millimolar range. J Neurophys 74, 2625–2637.
Ziv NE, Spira ME (1997). Localized and transient elevations of intracellular Ca2 +induce the dedifferentiation of axonal segments into growth cones. J Neurosci 17, 3568–3579.